GEOBRUGG®
BRUGG

Safety is our nature

Dimensioning and application of the flexible slope stabilization system **TECCO®** made from high-tensile steel wire mesh in combination with nailing and anchoring in soil and rock.

Technical Documentation (03/19)

TECCO® SYSTEM – PUBLICATIONS 1998-2019

TECCO® SYSTEM – SUMMARY OF PUBLISHED TECHNICAL PAPERS FROM 1998 UNTIL 2019.

A. Roduner, MSc Civil Eng.
Geobrugg AG
8590 Romanshorn, Switzerland
armin.roduner@geobrugg.com

THE DIMENSIONING AND APPLICATION OF THE FLEXIBLE SLOPE STABILIZATION SYSTEM TECCO® MADE FROM HIGH-TENSILE STEEL WIRE MESH IN COMBINATION WITH NAILING AND ANCHORING IN SOIL AND ROCK.

INTRODUCTION

Flexible slope stabilization systems made from wire meshes in combination with nailing are widely used in practice to stabilize soil and rock slopes. They are economical solutions and a good alternative to measures based on rigid concrete liner walls or massive supporting structures. Apart from designs using conventional steel wire, meshes from high-tensile steel wire are now also available on the market. The latter can absorb substantially higher forces and transfer them onto the nailing. Special concepts have been developed for the dimensioning of flexible slope stabilization systems for use on steep slopes in more or less homogeneous soil or heavily weathered loosened rock, but also on fissured and layered rock in which the bodies liable to break out are determined by fissure and layer surfaces. Stabilizations implemented in soil and rock, with and without vegetated face, confirm that these measures are suitable for practical application.

The use of flexible slope stabilization measures has proved its suitability in numerous cases and is often an alternative to massive concrete constructions. The open structure of the meshes, permits to realize a full-surface vegetation face. In most cases, wire meshes based on a tensile strength of the individual wires of $400-500 \, N/mm^2$ are used for slope stabilization purposes. If an economical spacing of the nails is aimed for, these simple meshes are often unable to absorb the occurring forces and to transmit them onto the nails.

The development of a wire mesh made from high-tensile steel wire of a tensile strength of the individual wire of at least $1{,}770 \, N/mm^2$ offers new possibilities for an efficient and economical stabilization of slopes. Adapted dimensioning models taking the statics of soil and rock into account serve to dimension these stabilizations.

Fig. 1: TECCO®-Mesh TECCO® G65/3 (other product types: TECCO® G45/2, TECCO® G65/4)

Fig. 2: TECCO® system spike plates: P25/34, P33/40 and P33/50 (not shown in this picture), and P66/50

TECCO® SYSTEM: THE HIGH-TENSILE SLOPE STABILIZATION SYSTEM.

In standard layout, the high-tensile steel wire mesh TECCO® for slope stabilization is made from a steel wire of 3 mm diameter which has an aluminium-zinc coating (GEOBRUGG SUPERCOATING®) for protection against corrosion. The diamond-shaped meshes measuring 83 mm x 143 mm are produced by single twisting. The TECCO® steel wire mesh provides a tensile strength of 150 kN/m. Thanks to its three-dimensional structure, the mesh clings to the soil in an ideal manner and, additionally, serves to optimally secure sprayed-on greening.
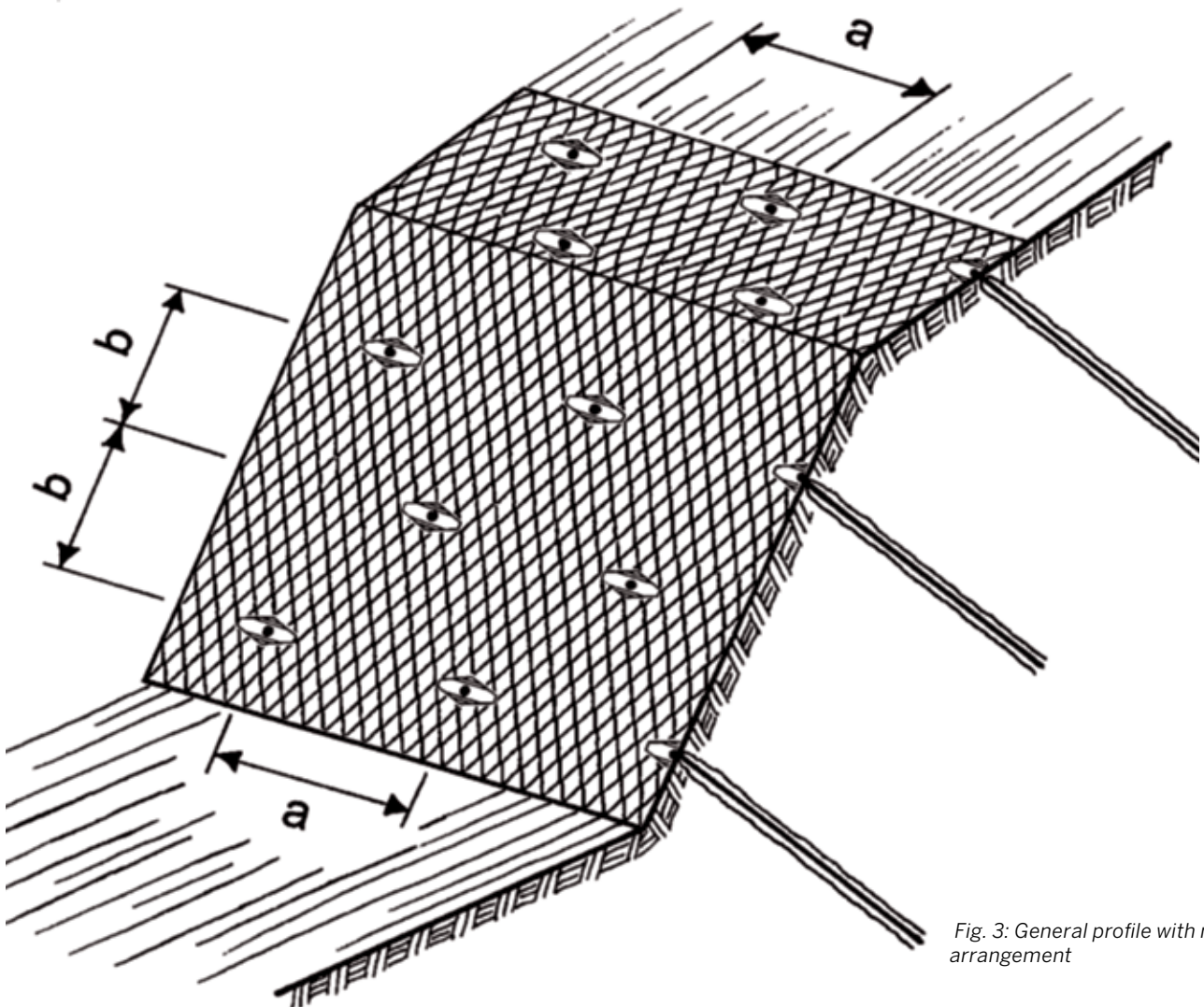

Fig. 3: General profile with nail arrangement

A SUCCESS STORY CONTINUES – JUST AS OUR MESHES ARE CONSTANTLY BEING FURTHER DEVELOPED.

The high-tensile steel wire mesh TECCO® has been developed by Geobrugg AG, Protection Systems, Romanshorn, Switzerland, primarily for stabilizing soil and rock slopes.

Substantially higher forces can be absorbed by this mesh in comparison with the wire mesh traditionally available on the market and offering a tensile strength in longitudinal direction of approximately 45–50 kN/m at comparable mesh size and similar wire diameter.

Special diamond-shaped system spike plates matching the TECCO® mesh serve to fix the mesh to soil or rock nails. By tightly pressing and if possible slightly impressing the spike plates in the ground to be stabilized, the mesh is tensioned in the best possible manner.

With the TECCO® slope stabilization system the rows of nails are offset to each other by half a horizontal nail distance. This means that the maximum possible local body liable to break out between the individual nails is limited to a width "a" and a length of 2 x"b".

Depending on the topographical or static conditions it is possible to optionally install boundary ropes to reinforce the rim areas. These boundary ropes are fixed to laterally positioned rope anchors and tensioned against these.

Fig. 4: Anzenwil, Switzerland

Fig. 5: Polymilou, Greece

Fig. 6: Implemented project in Japan

RUVOLUM® – THE DIMENSIONING CONCEPT FOR SOIL AND DECOMPOSED ROCK SLOPES.

The RUVOLUM® dimensioning concept serves to dimension slope stabilization systems which consist of a mesh cover in combination with nailing for soil and decomposed rock slopes. RUVOLUM® is in principle applicable to all slope stabilization systems commonly available on the market which allow flexible nail distance both horizontally and in line of slope.

The RUVOLUM® concept includes the investigation of superficial slope-parallel instabilities as well as the investigation of local instabilities between the individual nails.
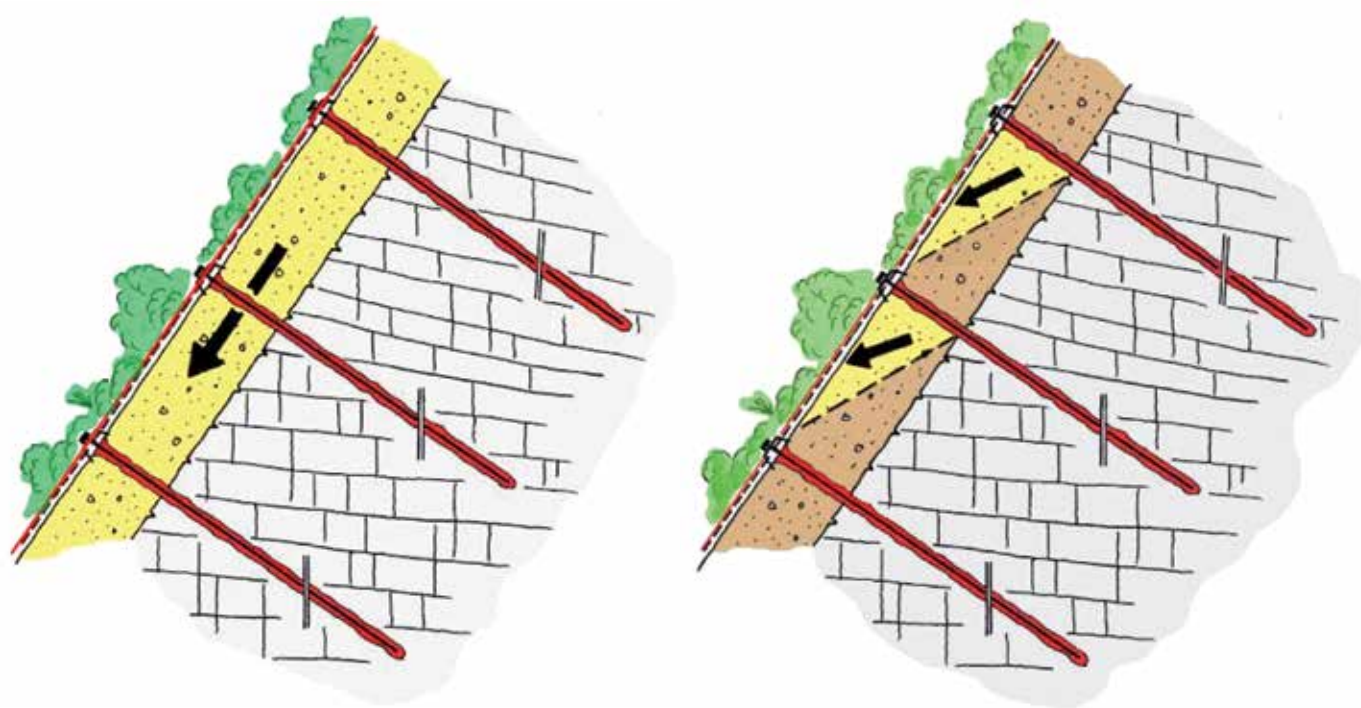

Fig. 7: Superficial slope-parallel instabilities and local instabilities between the individual nails

INVESTIGATION OF SUPERFICIAL SLOPE-PARALLEL INSTABILITIES.

The investigation of superficial slope-parallel instabilities concerns the cover layer which threatens to slide off the stable subsoil. The nailing is intended to stabilize the unstable cover layer as a whole. Hereby a cubic body of width **a**, length **b** and thickness **t** is fixed per nail with a certain safety.

Fig. 8 shows the forces acting on the body liable to break out which are taken into account. It is assumed that no excess hydrostatic pressure and no flow pressure is acting on the sliding body. Force **G** represents the dead weight of the cubic body. The term **c'·A** describes the retaining influence of the cohesion along the investigated sliding surface which is inclined by the angle α in relation to the horizontal plane. With **c'·A** it is also possible to, a.o., take into account an existing interlocking effect between the superficial layer to be protected and the stable subsoil, or within the superficial layer itself. Force V is a force with a stabilizing effect in the direction of the nail which pretensions the mesh against the slope surface. By tightening the nut, the spike plate and thereby the mesh is firmly pressed onto the ground. **V** is inclined in relation to the horizontal plane by the angle ψ. Variable **S** represents the shear force which is to be absorbed by the nail and transferred into the stable subsoil. Marked for completeness' sake are the reaction forces **N** and **T** from the sub-soil which act in vertical and tangential direction to the sliding surface.

From equilibrium considerations at the illustrated cubic body and taking into account the rupture condition of Mohr-Coulomb, one can, in function of the geometrical and geotechnical parameters as well as the pretension force **V** and the model uncertainty correction factor γ_{mod} formulate the general equation 1 for the stabilizing shear force **S**.
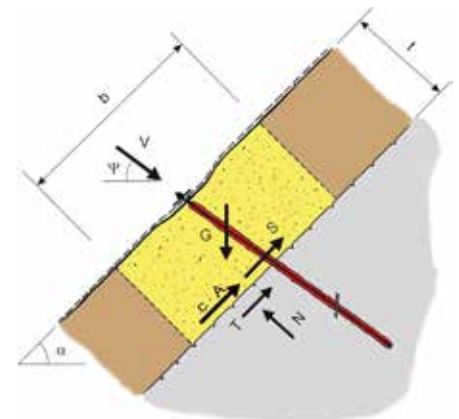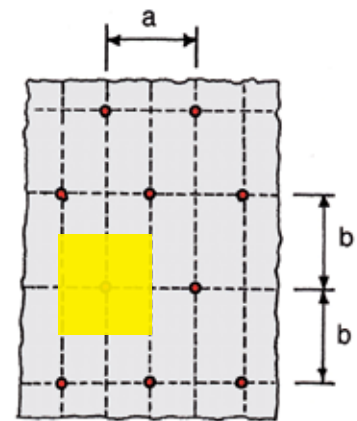

Fig. 8: Forces acting on the cubic body

Fig. 9: General nail arrangement

Equation 1

$$S \text{ [kN]} = 1/\gamma_{mod} \cdot \{\gamma_{mod} \cdot G \cdot \sin\alpha - V \cdot \gamma_{mod} \cdot \cos(\psi+\alpha)$$
$$- c' \cdot A - [G \cdot \cos\alpha + V \cdot \sin(\psi+\alpha)] \cdot \tan\varphi'\}$$

The RUVOLUM® dimensioning concept is using the concept with partial safety factors proclaimed in EUROCODE 7. The characteristic values of friction angle φ'_k, cohesion c'_k and volume weight γ_k are to be reduced or multiplied, respectively, by/with the corresponding partial safety correction values γ_φ, γ_c and γ_γ (whereby the friction angle φ'_k is reduced via the tangent).

The following three proofs of bearing safety must be established in the context of the investigation of superficial slope-parallel instabilities:

1. Proof against a superficial layer sliding-off
2. Proof of the mesh against puncturing
3. Proof of the nail to combined stress

Proof against sliding-off of a superficial layer parallel to the slope
In the proof against a superficial layer parallel to the slope sliding-off it must be guaranteed that the cubic body of width **a**, length **b** and thickness **t** does not slide off the investigated sliding surface which is inclined by the angle α in relation to the horizontal plane.

The mathematically required shear force S_d at dimensioning level, determined according to equation 1, must be compared with the bearing resistance S_R of the nail in respect of pure shear stress, whereby the resistance correction value γ_{SR} for shearing off of the nail must be considered. Proof of bearing safety is to be established as follows:

$$S_d \leq S_R / \gamma_{SR}$$

S_d = Dimensioning value of the shear stress under consideration of the dimensioning values of the geotechnical parameters and of the external, stabilizing force V_{d1} at dimensioning level, whereby the following applies:

$V_{d1} = V \cdot \gamma_{d1}$ (V_{d1} acts favourably on force S_d, consequently $\gamma_{d1} = 0.80$ is generally taken)

S_R = Bearing resistance of the nail to shear stress, whereby the following applies:

$S_R = \tau_y \cdot A$ with $\tau_y = f_y / \sqrt{3}$ = yield point under shear stress, f_y = yield point under tensile stress, A = statically effective cross-section of the nail

γ_{SR} = Resistance correction value. Based on EUROCODE 7, $\gamma_{SR} = 1.50$ is generally taken or assumed

Proof of the mesh against puncturing
In the proof of the mesh against puncturing it must be investigated whether or not the mesh is able to absorb the force **V** applied in nail direction, and transfer it into the stable subsoil. Hereby the dimensioning value of the externally applied force **V** is compared with the bearing resistance of the mesh to pressure stress in nail direction, whereby the resistance correction value for puncturing is taken into account. Proof of bearing safety must be established as follows:

$$V_{d2} \leq D_R / \gamma_{DR}$$

V_{d2} = Dimensioning value of the external force **V** with which the slope stabilization system is pretensioned against the nails. The following applies:

$V_{d2} = V \cdot \gamma_{V2}$ with $\gamma_{V2} = 1.50$ (as leading influence)

D_R = Bearing resistance of the mesh against pressure stress in nail direction; to be determined by tests developed specifically for the purpose

γ_{DR} = Resistance correction value, generally $\gamma_{DR} = 1.50$ is taken

Proof of the nail to combined stress

The nail is subjected to tensile stress by the effectively applied pretension force. Additionally, the nail must prevent a slope-parallel sliding-off of a layer of thickness **t** close to the surface, which subjects it to shear stress. With the proof of the nail's bearing safety it must be investigated whether or not the nail is able to absorb these combined stress. Proof of bearing safety is to be established as follows:

$$\sqrt{[V_{d2} / (T_R / \gamma_{VR})]^2 + [S_d / (S_R / \gamma_{SR})]^2} \leq 1.0$$

V_{d2} = Dimensioning value of the external force V with which the slope stabilization system is pretensioned against the subsoil.

The following applies: $V_{d2} = V \cdot \gamma_{V2}$ with $\gamma_{V2} = 1.50$

T_R = Bearing resistance of the nail to pure tensile stress, whereby the following applies:

$T_R = f_y \cdot A$ with f_y = yield point under tensile stress,
A = statically effective nail cross-section

γ_{VR} = Resistance correction value, based on EUROCODE 7, is generally taken as $\gamma_{VR} = 1.50$

S_d = Dimensioning value of the shear stress under consideration of the dimensioning values of the geotechnical parameters and of the external, stabilizing force V_{d1} at dimensioning level, whereby the following applies:

$V_{d1} = V \cdot \gamma_{d1}$ (V_{d1} acts favourable on force S_d, consequently $\gamma_{d1} = 0.80$ is generally taken)

S_R = Bearing resistance of nail to shear stress, whereby the following applies:

$S_R = \tau_y \cdot A$ with $\tau_y = fy / \sqrt{3}$ = yield point under shear stress,
f_y = yield point under tensile stress, A = statically effective cross-section of nail

γ_{SR} = Resistance correction value. Based on EUROCODE 7, $\gamma_{SR} = 1.50$ is generally taken

INVESTIGATION OF LOCAL INSTABILITIES BETWEEN THE INDIVIDUAL NAILS.

Fig. 10: Local instabilities between the individual nails

Fig. 11: General nail arrangement

Fig. 12: Cross-section of the maximum possible body liable to break out, of thickness t; actively stabilized truncated pressure cones laterally

The second investigation looks at bodies liable to break out locally, between the individual nails. The slope stabilization system "Nailing in combination with a mesh cover" is to be dimensioned in such a manner that all possible local bodies liable to break are retained, the maximum occurring forces absorbed and transmitted into the stable subsoil. In the investigation of local bodies liable to break out between the nails, one must reflect which bodies become possible, taking into account the chosen nail arrangement. Above each nail is a field of width a and length $2 \cdot b$ which must be secured against local instabilities. Starting from this field, bodies liable to break out of a maximum length of $2 \cdot b$ can arise.

The cross-section of the maximum possible wedge liable to break out is substantially influenced by the actual protection concept. The mesh is pre-tensioned against the slope surface with the force V in that tightening of the nut causes the spike plate to be pressed firmly onto or even slightly into the ground.
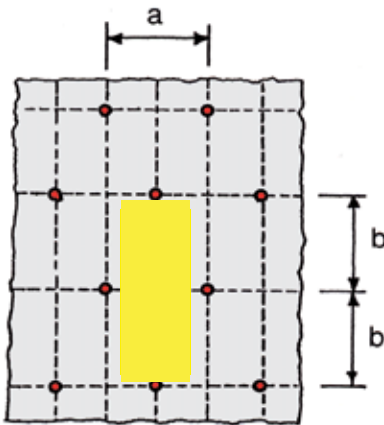
Starting from the nail head, a truncated pressure cone arises in the cover layer below the spike plate and the adjoining mesh. This cone can be described by the geometrical parameters ζ, ξ and t. The angle δ represents the inclination of the truncated cone relative to the horizontal plane.

The variable ζ_{min} depends on the applied spike plate, the mesh and the ground, and must be determined by means of tests. As a simplifying assumption, $\zeta_{min} = 0.5 \cdot D_{Plate}$ can be assumed.

The dimensioning model assumes that the pressure cones are completely outside the body to be investigated. This means that the cross-section of the maximum possible body liable to break out is trapezoidal and features at the top a width of $(a - 2 \cdot \zeta)$ and at the bottom a width of $(a - 2 \cdot \xi = \eta)$, and at the bottom a width of $a_{red} = (a - t / \tan\delta - 2 \cdot \zeta)$ and thickness t (cf. fig. 12).
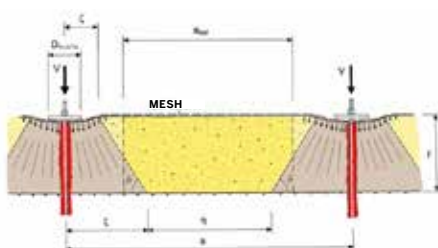
The body liable to break out and subject of the investigation features a width of a_{red} and a maximum length of $2 \cdot b$. The thickness of the body in Fig. 11 amounts to t. For the proofs of bearing safety in the investigation of local instabilities according to the dimensioning method described in this chapter, it is mandatory to vary the thickness of the bodies to be investigated over the entire interval [0;t] and in this manner to determine the decisive fault mechanism. Hereby it must be noted that the variable a_{red} depends directly on the thickness of the investigated body liable to break out and accordingly also varies on variation of the layer thickness from 0 to t.

If the layer thickness is not varied between 0 and t, this can lead to a substantial underestimation of the effectively occurring forces, particularly if t is selected greater than 1/2 - 1/3 of the distance between nails in the line of slope. In the interest of simplification, only the case thickness of the layer = t is dealt with in the explanations hereafter.

It must be pointed out that the geometry of the bodies to be investigated and selected in the model should approximately simulate the saucer-shaped fault contours which occur in reality. By the trapezoidal cross-section the actually curved cross-section is described as an approximation.

For the proofs of bearing safety in the investigation of local instabilities, one must differentiate between two fault mechanisms **A** and **B**: mechanism **A** represents a single-body sliding mechanism whose sliding surface, starting from the bottom nail, runs in a straight line to the top nail under the angle β in relation to the horizontal plane. Fault mechanism **B** is a two-body sliding mechanism. Hereby the top body **I** of trapezoidal cross-section presses on the wedge-shaped bottom body **II**. Figs. 13 and 14 illustrate these two possible fault mechanisms with the acting forces accordingly.
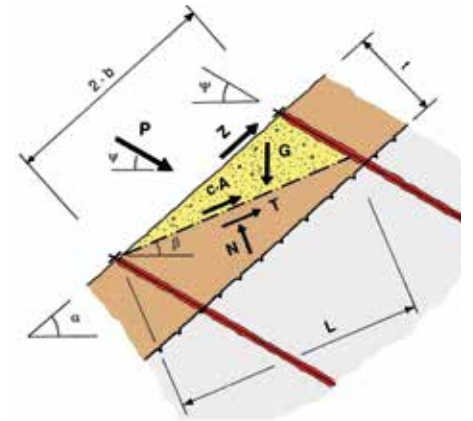

Fig. 13: Fault mechanism A

Fault mechanism A
In the investigation of local instabilities with the aid of fault mechanism **A**, we look at a wedge-shaped body of width a_{red} which threatens to slide off a plane which is inclined in relation to the horizontal plane by the angle β. All considered forces which are active on the sliding body are marked in Fig. 13. Hereby it is assumed, in analogy to the investigation of superficial slope-parallel instabilities, that no excess hydrostatic pressure, no flow pressure and no accelerations due to earthquake acts on the sliding body (this applies also to fault mechanism **B**). Force **G** represents the dead weight of the body breaking out. The cohesion along the sliding surface is taken into account with the term **c' · A**, whereby $A = L \cdot a_{red}$ applies. With **c' · A** it is in turn possible to describe an existing interlocking effect.

Also active on the body liable to break out, furthermore, are the external forces **P** und **Z** with a stabilizing effect. It is assumed that the investigated body liable to break out and wanting to move relatively downwards, is partly retained via friction by the mesh pressed onto the surface. If these friction forces are integrated over the surface $2b \cdot a_{red}$, the resulting reaction is the slope-parallel upwards-directed force **Z** in the mesh, which is to be selectively transmitted by the mesh to the upper nail. Force **P** is assumed to be inclined in relation to the horizontal plane by the angle Ψ and is introduced as a general force required from the equilibrium considerations and having a stabilizing effect. For completeness' sake, the reaction forces **N** und **T** from the subsoil, acting in vertical or tangential direction in relation to the sliding surface, are also marked. The relation presented in equation 2 results from equilibrium considerations and taking into account the rupture condition of Mohr-Coulomb as well as the model uncertainty correction factor γ_{mod}. The maximum force **P** is to be mod determined by variation of the inclination of sliding surface β.

Equation 2

$$P \text{ [kN]} = \frac{G \cdot [\gamma_{mod} \cdot \sin\beta - \cos\beta \cdot \tan\varphi'] - \ldots}{\gamma_{mod} \cdot \cos(\beta+\Psi) + \sin(\beta+\Psi) \cdot \tan\varphi'}$$

$$\frac{Z \cdot [\gamma_{mod} \cdot \cos(\alpha-\beta) - \sin(\alpha-\beta) \cdot \tan\varphi'] - c' \cdot A}{\gamma_{mod} \cdot \cos(\beta+\Psi) + \sin(\beta+\Psi) \cdot \tan\varphi'}$$
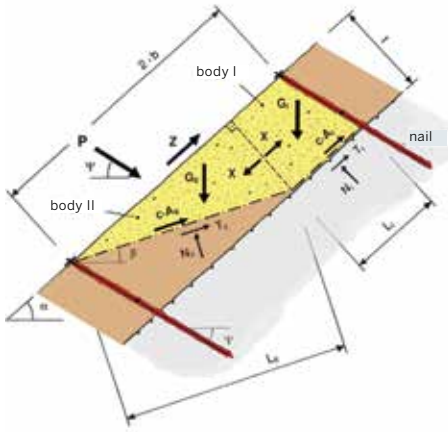
Fig. 14: Fault mechanism B (possible friction forces along the contact surface between the two bodies I and II are neglected)

Fault mechanism B

Fault mechanism **B** is characterized by two bodies liable to break out: The upper, trapezoidal body **I** presses over the contact force X onto the lower, wedge-shaped body **II**. The width of the two bodies amounts to a_{red}. The forces G_I and G_{II} represent the weights of the individual sliding bodies and **c' · A$_I$** and **c' · A$_{II}$** respectively, the forces due to cohesion along the investigated sliding surfaces of the individual sliding bodies, whereby $A_I = L_I \cdot a_{red}$ and $A_{II} = L_{II} \cdot a_{red}$ apply. N_I and T_I and N_{II} and T_{II} respectively, in turn stand for the reaction forces from the subsoil. Analogously to the preceding paragraph, variable **Z** denotes the slope-parallel force in the mesh, to be selectively transmitted on the upper nail. The force **P** is assumed to be inclined in relation to the horizontal plane by the angle Ψ and is again introduced as a general retaining force required from the equilibrium considerations. For the equilibrium equations, the forces Z and P should act on the lower wedge-shaped body II.

The contact force **X** results from the equilibrium equations at the upper body **I**, whereby the condition of Mohr-Coulomb and the model uncertainty correction factor γ_{mod} are taken into account. To determine the force **P**, the equilibrium conditions are formulated on body **II**. Hereby the contact force **X** from equation 3 and the slope-parallel force **Z** are entered.

The decisive case is to be found by comparing the maximum force **P** from mechanism **A** with that from mechanism **B**.

Equation 3

$$X\ [kN] = 1/\gamma_{mod} \bullet \{G_I \bullet (\gamma_{mod} \bullet \sin\alpha - \cos\alpha \bullet \tan\varphi') - c' \bullet A_I$$

Equation 4

$$P\ [kN] = \frac{G_{II} \bullet [\gamma_{mod} \bullet \sin\beta - \cos\beta \bullet \tan\varphi'] - ...}{\gamma_{mod} \bullet \cos(\beta+\Psi) + \sin(\beta+\Psi) \bullet \tan\varphi'}$$

$$\frac{(X - Z) \bullet [\gamma_{mod} \bullet \cos(\alpha-\beta) - \sin(\alpha-\beta) \bullet \tan\varphi'] - c' \bullet A_{II}}{\gamma_{mod} \bullet \cos(\beta+\Psi) + \sin(\beta+\Psi) \bullet \tan\varphi'}$$

The following two proofs of bearing safety must be submitted as far as the investigation of local instabilities between the individual nails is concerned:

1. Proof of the mesh against shearing-off at the up-slope edge of the spike plate

2. Proof of the mesh to selective transmission of the slope-parallel force **Z** onto the upper nail

Proof of the mesh against shearing-off at the upslope edge of the spike plate at lower nail

In the investigation of local instabilities it must be guaranteed that a local body of a maximum length of **2 · b** cannot break out of the superficial layer to be stabilized. For this purpose the retaining force P required from the equilibrium conditions has been determined. If the investigated body liable to break out threatens to slide off, it presses outwards in the area of the lower nail with this maximum force **P**. The mesh must be sufficiently strong to withstand this shear stress and to carry the force **P** away over the spike plate onto the nail.

In the proof of the mesh against shearing-off at the up-slope edge of the spike plate at the lower nail, it must be investigated whether the applied mesh is able to absorb the force **P** acting outwards in the direction of the nail or shear at the upslope edge of the spike plate. Proof of bearing safety must be established as follows:

$$P_d \leq P_R \,/\, \gamma_{PR}$$

P_d = Dimensioning value of the maximum shear stress on the mesh at the upslope edge of the spike plate on the lower nail

P_R = Bearing resistance of the mesh against shearing-off in nail direction, to be determined by means of the test developed specifically for the purpose

γ_{PR} = Resistance correction value, γ_{PR} = 1.50 is generally assumed

Proof of the mesh to selective transmission of the slope-parallel force Z onto the upper nail

The slope parallel force **Z** has been brought in for the equilibrium considerations. This force **Z** must be transmitted selectively from the mesh over the spike plate onto the upper nail. Proof of bearing safety concerning the selective transmission of the force **Z** from the mesh onto the upper nail must be established as follows:

$$Z_d \leq Z_R \,/\, \gamma_{ZR}$$

Z_d = Slope-parallel force taken into account in the equilibrium equations = dimensioning value of the stress in slope-parallel direction

Z_R = Bearing resistance of the mesh against selective, slope-parallel tensile stress; to be determined by tests developed specifically for the purpose

γ_{ZR} = Resistance correction value, γ_{ZR} = 1.50 is generally assumed

DIMENSIONING EXAMPLE

An example for the investigation of superficial instabilities is to demonstrate the application of the RUVOLUM® concept, for example for dimensioning the flexible slope stabilization system TECCO®. Hereby it is assumed that the stable subsoil (rock) is covered by a soil layer (sandy gravel) of thickness t which must be protected against instabilities. All necessary geometrical and geotechnical input data are compiled in the table below.

Table 1: System elements considered in the dimensioning example

System elements
High-tensile steel wire mesh TECCO® G65/3
TECCO® system spike plate
Nail type GEWI D = 28 mm
(Rusting away of the nail taken into account: diameter reduced by 4 mm)

Table 2: Input data for the example to dimension the TECCO® system slope stabilization

Input data	Abbreviation	Values
Slope inclination	α [degrees]	60.0
Layer thickness	t [m]	0.50 / 1.00
Friction angle ground (characteristic value)	φ' [degrees]	35.0
Cohesion ground (characteristic value)	c' [kN /m²]	0.0
Volume weight ground (characteristic value)	γ [kN /m³]	22.0
Partial safety correct. value friction angle	γ_{φ} [-]	1.25
Partial safety correct. value cohesion	γ_c [-]	1.25
Partial safety correct. value volume weight	γ_{γ} [-]	1.00
Model uncertainty correction value	γ_{mod} [-]	1.10
Slope-parallel force	Z_d [kN]	15.0
Preload force of the system	V [kN]	30.0
Nail inclination to horizontal	ψ [degrees]	25.0

Taking into account the system elements compiled in table 1 and the input quantities compiled in table 2, the dimensioning calculation results in the maximum possible distance a (horizontally), and b (in the line of slope):

for t = 0.50 m: a = b = 3.00 m
for t = 1.00 m: a = b = 2.65 m

If the layer thickness is t = 0.50 m, the mesh becomes decisive. Hereby the proof of the mesh against shearing-off at the upslope edge of the spike plate is the determining proof of bearing safety, as compiled in table 3.

Quantities	Abbreviation	Values
Dimensioning value of the max. stress on the mesh for shearing-off at the upslope edge of the spike plate at the lower nail	P_d [kN]	58.6
Bearing resistance of the mesh against shearing-off in nail direction at the up-slope edge of the spike plate (determined in tests)	P_R [kN]	90.0
Resistance correction value for shearing of the mesh	γ_{PR}[-]	1.5
Dimensioning value of the bearing resistance of the mesh against shearing-off	P_R / γ_{PR} [kN]	60.0
Proof of bearing safety	$P_d \leq\, = P_R / \gamma_{PR}$	fulfilled

Table 3: Decisive proof of the mesh bearing safety against shearing off at the edge of spike plate for layer thickness t = 0.50 m

In case of a layer thickness **t** = 1.00 m it is no longer the mesh which is decisive in the dimensioning example, but the nail, whereby the mesh is utilized in optimal manner. The determining proof of bearing safety in this case is the proof of the nail against a slope-parallel sliding-off of the surface layer. This is compiled in table 4.

Quantities	Abbreviation	Values
Preload force effectively applied on nail	V [kN]	30.0
Load factor for positive influence of pretension V	$\gamma\, V_I$ [-]	0.8
Dimensioning value of the applied preload force by positive influence of V	V_{dI} [kN]	24.0
Load factor for negative influence of pretension V	$\gamma\, V_{II}$[-]	1.5
Dimensioning value of the applied preload force by negative influence of V	V_{dII} [kN]	45.0
Calculated required shear force at dimensioning level in function of V	S_d [kN]	80.2
Max. stress on the mesh for shearing-off	P_d [kN]	42.0
Bearing resistance of the nail to tensile stress	T_{Rred} [kN]	226.0
Bearing resistance of the nail to shear stress	S_{Rred} [kN]	131.0
Resistance correction value for tensile stress	γ_{TR}[-]	1.5
Resistance correction value for shear stress	γ_{SR}[-]	1.5
Proof of bearing safety: $\{(V_{dII} / (T_{Rred} / \gamma_{TR}))^2+ (S_d / (S_{Rred} / \gamma_{SR}))^2\}^{0.5} <= 1.0$	0.966 <=1.0	fulfilled
Proof of bearing safety: $\{(P_d / (T_{Rred} / \gamma_{TR}))^2+ (S_d / (S_{Rred} / \gamma_{SR}))^2\}^{0.5} <= 1.0$	0.960 <=1.0	fulfilled

Table 4: Proof of the nail to combined stress

LOAD CASE "EARTHQUAKE"

Depending on the importance of the structure and the seismological situation, possible additional effects from earthquakes must be investigated when dimensioning slope stabilization systems. Generally this takes place using the substitute force procedure. Here, accelerations acting on a fracture body are converted through the factors ε_h and ε_v to additional forces in the horizontal and vertical direction. These additional forces must be appropriately taken into account in the equilibrium considerations. With steeper slopes, in general in solid rock, special investigations are necessary e.g. tilting and sliding individual blocks.

Shown below are the additions in the formulas resulting from the earthquake load case. The corresponding individual proofs remain the same as previously described.
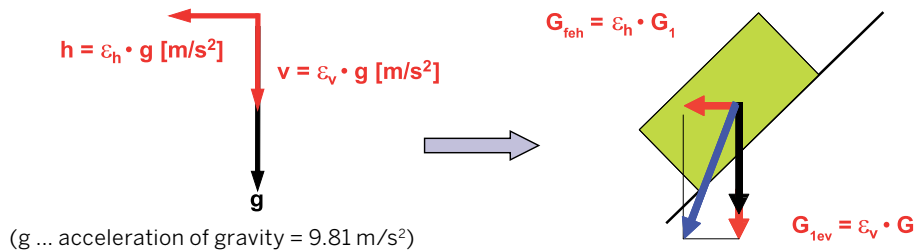
$$h = \varepsilon_h \cdot g \ [m/s^2]$$

$$v = \varepsilon_v \cdot g \ [m/s^2]$$

$$g$$

$$G_{feh} = \varepsilon_h \cdot G_1$$

$$G_{1ev} = \varepsilon_v \cdot G$$

(g ... acceleration of gravity = 9.81 m/s²)

Fig. 15: Components of acceleration due to earthquake

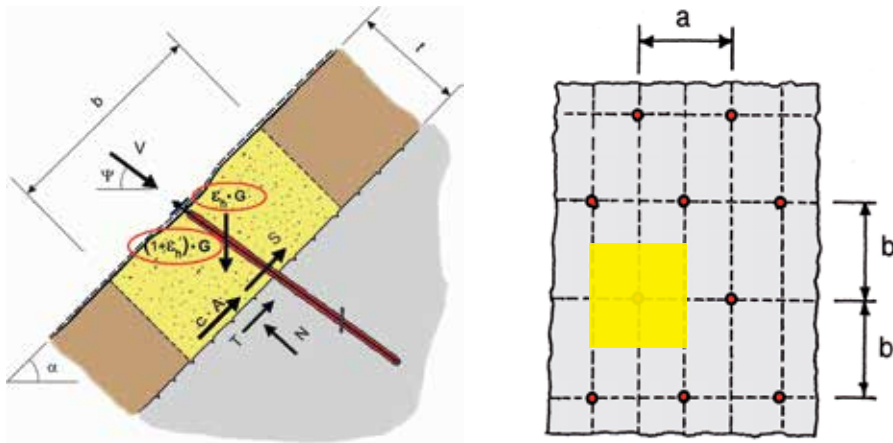## Investigation of instabilities close to the surface and parallel to the slope

Fig. 16: All forces applied to a cubic body with the earthquake load case

The formula for the variable **S** previously described in equation 1 is extended in equation 5 with the additional forces as a result of the parameters ε_h and ε_v – factors of the horizontal and vertical acceleration as the result of an earthquake. Here the variable S represents the shear force to be taken up by the nail and transferred to the firm bedrock.
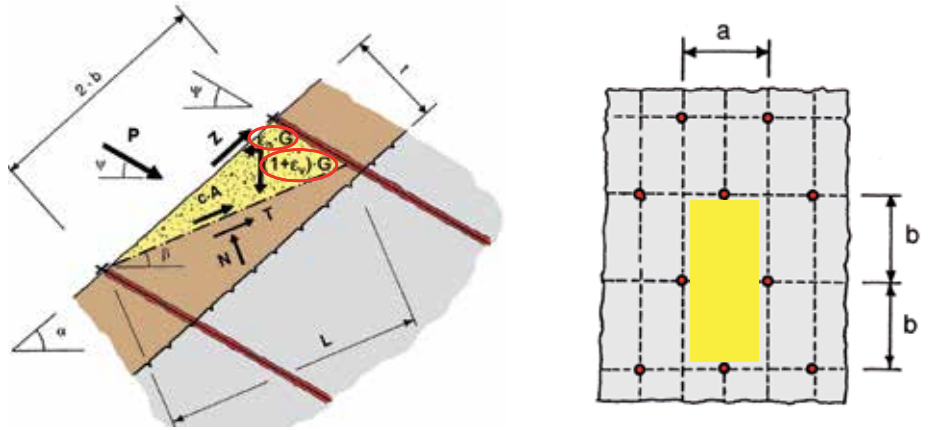
Equation 5

$$S \ [kN] = (1+\varepsilon_v) \cdot G \cdot \sin\alpha + \varepsilon_h \cdot G \cdot \cos\alpha - V \cdot \cos(\Psi+\alpha) - \frac{[V \cdot \sin(\Psi+\alpha) + (1+\varepsilon_v) \, G \cdot \cos\alpha - \varepsilon_h \cdot G \cdot \sin\alpha] \cdot \tan\varphi + c \cdot A}{\gamma_{mod}}$$

Investigation of local instabilities between the nails

Break mechanism A

Fig. 17: All forces applied with break mechanism A including the earthquake load case

The additional force components as a result of earthquake are introduced in the equilibrium consideration previously described with equation 2 (see equation 6). Here the variables **P** and **Z** represent the external stabilizing forces. The inclination β of the slip surface must in turn be varied in order to determine the maximum force **P**.

Equation 6

$$P \text{ [kN]} = \frac{(1+\varepsilon_v) \cdot G \cdot \sin\beta + \varepsilon_h \cdot G \cdot \cos\beta - Z \cdot \cos(\alpha-\beta) - \dfrac{[(1+\varepsilon_v) \, G \cdot \cos\beta - \varepsilon_h \cdot G \cdot \sin\beta - Z \cdot \sin(\alpha-\beta)] \cdot \tan\varphi + c \cdot A_c}{\gamma_{mod}}}{\cos(\Psi+\beta) + \sin(\Psi+\beta) \cdot \dfrac{\tan\varphi}{\gamma_{mod}}}$$
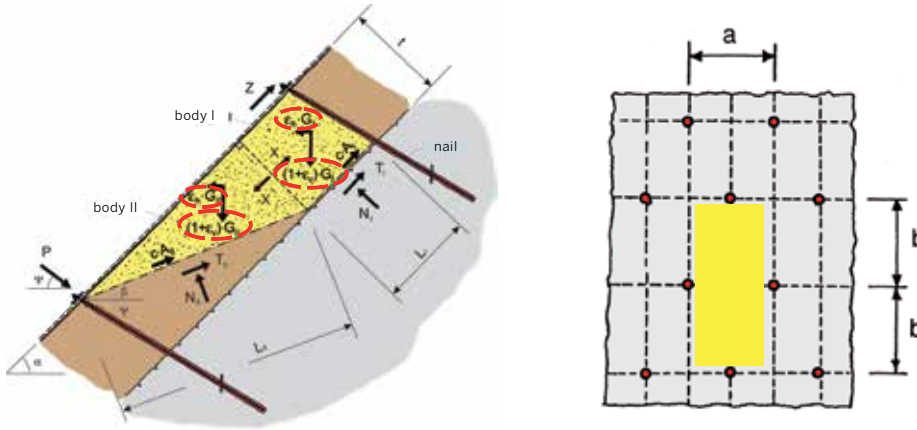
Break mechanism B

Fig. 18: All forces applied with break mechanism A including the earthquake load case

The additional force components as a result of earthquake are likewise introduced with fracture mechanism B. For this the contact force **X** of equation 3 resulting from the equilibrium considerations at the upper body I must be adjusted as represented in equation 7. Shown in equation 8 is the extended calculation of the necessary restraining force **P**.

By analogy with before, the decisive case must also be determined with the maximum force **P** from mechanism A and B.

Equation 7: Contact force X

$$X \, [kN] = (1+\varepsilon_V) \cdot G_I \cdot \sin\alpha + \varepsilon_h \cdot G_I \cdot \cos\alpha - \frac{[(1+\varepsilon_V) \cdot G_I \cdot \cos\alpha - \varepsilon_h \cdot G_I \cdot \sin\alpha] \cdot \tan\varphi + c \cdot A_{c,\,I}}{\gamma_{mod}}$$

Equation 8: Retaining force P

$$P \, [kN] = \frac{(1+\varepsilon_V) \cdot G_{II} \cdot \sin\beta + \varepsilon_h \cdot G_{II} \cdot \cos\beta + X \cdot \cos(\alpha-\beta) - Z \cdot \cos(\alpha-\beta) - \dfrac{[(1+\varepsilon_V) \, G_{II} \cdot \cos\beta - \varepsilon_h \cdot G_{II} \cdot \sin\beta - Z \cdot \sin(\alpha-\beta) + X \cdot \sin(\alpha-\beta)] \cdot \tan\varphi + c \cdot A_{II}}{\gamma_{mod}}}{\cos(\Psi+\beta) + \sin(\Psi+\beta) \cdot \dfrac{\tan\varphi}{\gamma_{mod}}}$$

LOAD CASE "STREAMING PARALLEL TO THE SLOPE"

Described below is the influence of streaming pressure as a result of precipitation water, respectively inflowing ground or slope water in loose rock slopes in the equilibrium considerations. In principle the two types of inflow with precipitation water (from the outside on to the slope) and slope water (from the inside) can be differentiated as shown in Fig. 19. With both cases it is assumed that a streaming parallel to the slope occurs after the saturation of the material.

Fig. 19: Streaming parallel to the slope in the case of intensive rain (left) and slope water, e.g. in waterbearing interbeds, clefts etc. (right)
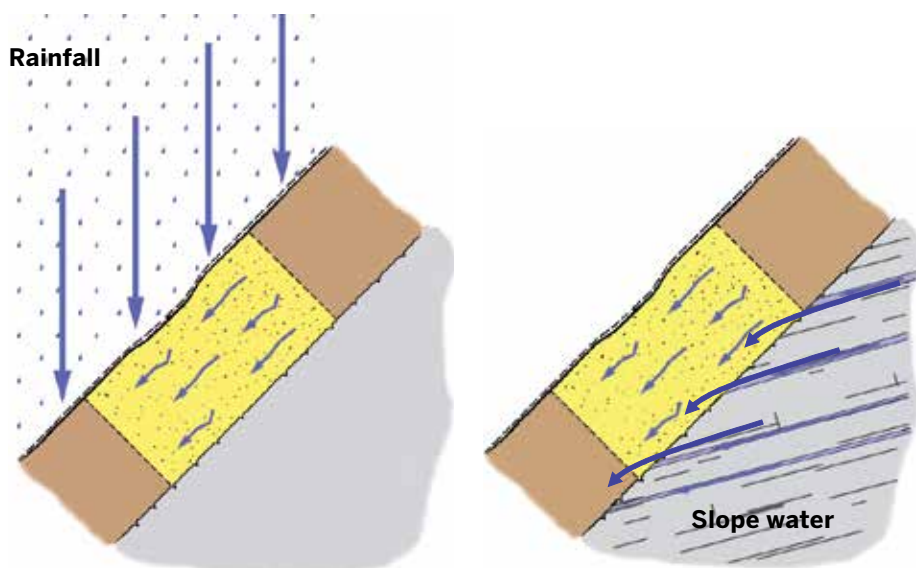
Investigation of instabilities close to the surface and parallel to the slope

The additional force F_s represents the resulting streaming force parallel to the slope and is calculated from the sum of the unit weight of the water (γ_w), the hydraulic gradient ($i = \sin \alpha$) and the volume of the fracture body (V). When calculating according to equation 9, buoyancy is taken into account with the own weight G of the cubic body. The individual proofs remain the same as previously stated.
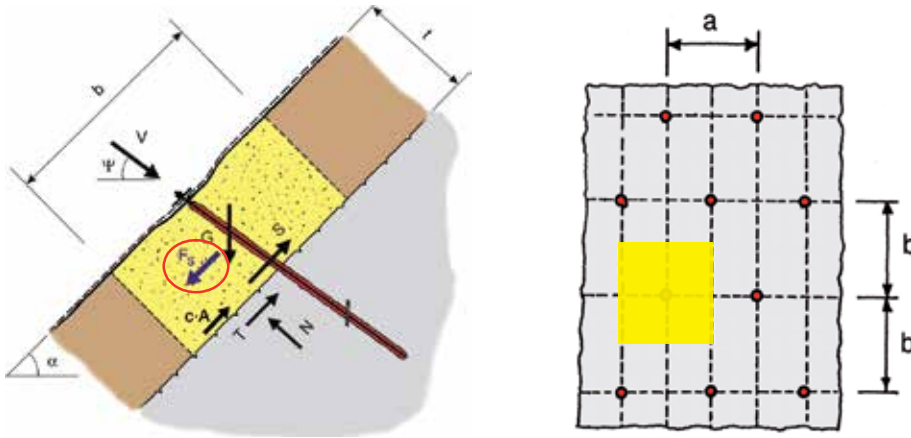

Fig. 20 : All forces applied to a cubic body including the streaming load case,

The general shear force formula S, previously represented in equation 1 is extended by the force F_s.

$$S \text{ [kN]} = G \cdot \sin\alpha - V \cdot \cos(\Psi+\alpha) + F_S - \frac{[V \cdot \sin(\Psi+\alpha) + G \cdot \cos\alpha] \cdot \tan\varphi + c \cdot A}{\gamma_{mod}}$$

Equation 9: Shear force S

Investigation of local instabilities between the nails
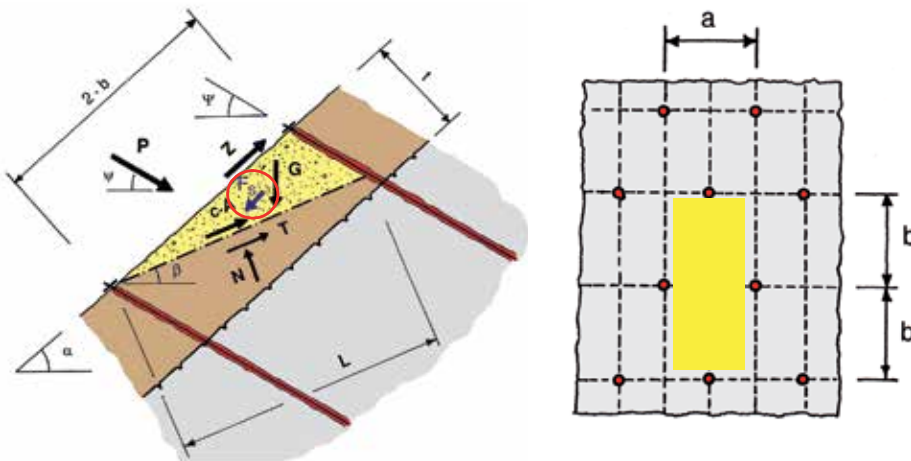
Break mechanism A

Fig. 21: All forces applied with the break mechanism including the streaming load case

The equation for calculating stabilizing force P is enlarged by the force components F_s. The maximum force P is determined by varying the gradient β of the slip face. The uplift is taken into account with the calculation of the own weight G.

Equation 10 : Restraining force P

$$P \text{ [kN]} = \frac{F_S \cdot \cos(\alpha-\beta) + G \cdot \sin\beta - Z \cdot \cos(\alpha-\beta) - \dfrac{[G \cdot \cos\beta - Z \cdot \sin(\alpha-\beta) + F_S \cdot \sin(\alpha-\beta)] \cdot \tan\varphi + c \cdot A_c}{\gamma_{mod}}}{\cos(\Psi+\beta) + \sin(\Psi+\beta) \cdot \dfrac{\tan\varphi}{\gamma_{mod}}}$$

Break mechanism B

Fig. 22: All forces applied with the break mechanism including the streaming load case
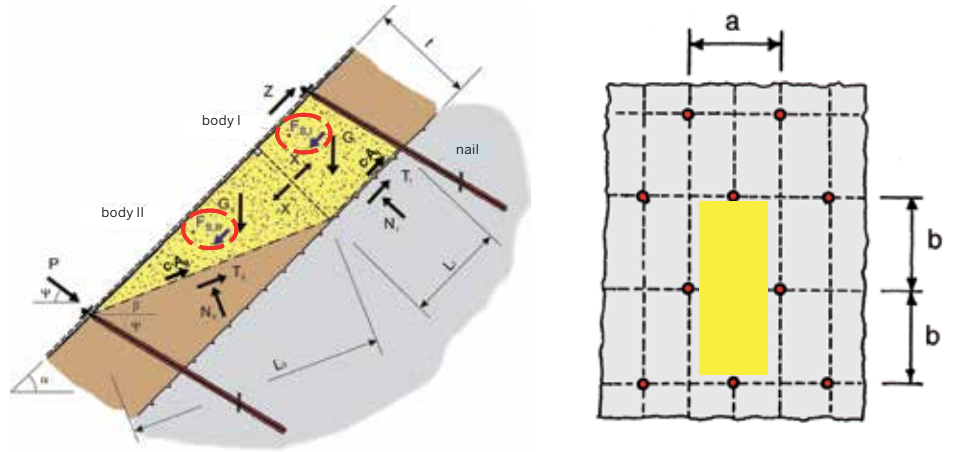
According to the equilibrium consideration, at the upper body I the contact force **X** of equation 3 is extended by the force $F_{s,I}$. Represented in equation 12 is the extended calculation of the restraining force **P** The own weight **G** is thereby reduced by the uplift components.

The maximum force **P** from the two fracture mechanisms A and B is determining for the proofs.

Equation 11: Contact force X

$$X \, [kN] = F_{S,I} + G_I \cdot \sin\alpha - \frac{G_I \cdot \cos\alpha \cdot \tan\varphi + c \cdot A_{c,I}}{\gamma_{mod}}$$

Equation 12: Restraining force P

$$P \, [kN] = \frac{G_{II} \cdot \sin\beta + X \cdot \cos(\alpha-\beta) + F_{S,II} \cdot \cos(\alpha-\beta) - Z \cdot \cos(\alpha-\beta) - \dfrac{[G_{II} \cdot \cos\beta - Z \cdot \sin(\alpha-\beta) + X \cdot \sin(\alpha-\beta) + F_{S,II} \cdot \sin(\alpha-\beta)] \cdot \tan\varphi + c \cdot A_{C,II}}{\gamma_{mod}}}{\cos(\Psi+\beta) + \sin(\Psi+\beta) \cdot \dfrac{\tan\varphi}{\gamma_{mod}}}$$
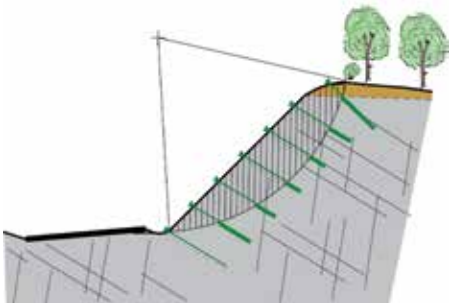
Fig. 23: Investigation of the overall stability

Fig. 24: Sliding-block method

INVESTIGATION OF THE GLOBAL STABILITY
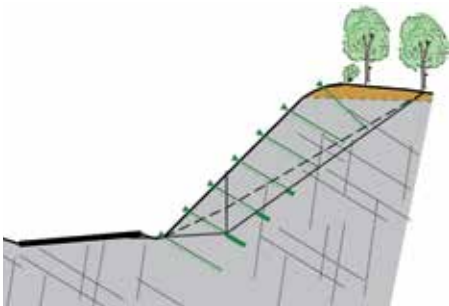
In addition to the investigations of instabilities near the surface according to the RUVOLUM® concept, the investigation of the overall stability with deep sliding surfaces must also be established depending on the prevailing subsoil and stability circumstances. The relevant calculations are carried out according to conventional methods of stability investigation, for example with curved sliding surfaces in soil or decomposed rock, respectively, or according to the sliding-block method where sliding surfaces marked by stratification, fissures are concerned.

For the investigation of the overall stability, the nails are generally introduced as tension elements. By checking the internal bearing resistances (steel cross-sections and yield point under tensile load of the nails) and the external bearing resistances (friction forces that can be mobilized, maximum head force D_{max} that can be mobilized as per Fig. 26), the terrain's resistance against sliding η and the utilization factor $1/f$ of the existing shear and system resistances are determined.

The tensile resistance available at the intersection between sliding surface and nail is limited by:

1. the internal bearing resistance of the nail: Z_i
2. the external bearing resistance behind the sliding surface: $Z_{AH} = \tau_2 \cdot l_2$
3. the external bearing resistance ahead of the sliding surface plus the system or the maximum head force that can be mobilized in case of a failure of the system against puncturing
   $$Z_{AVmax} = \tau_1 \cdot l_1 + D_{max}$$

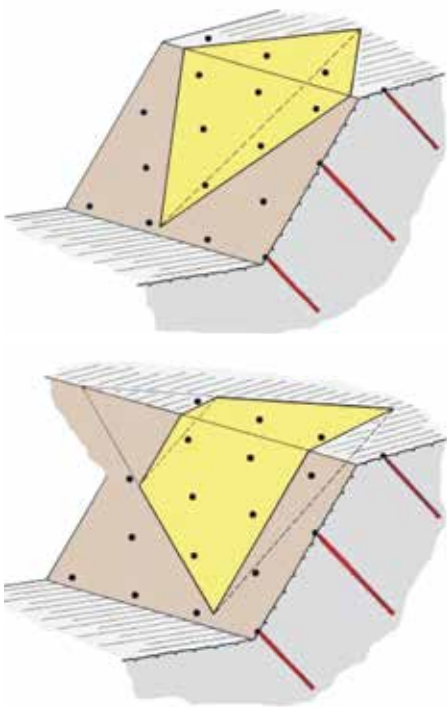whereby the smallest of the values Z_i, Z_{AH} and Z_{AVmax} is decisive.

Fig. 25 (above): Wedge-shaped body liable to break out, extending over the entire slope and reaching clearly beyond the edge of the slope
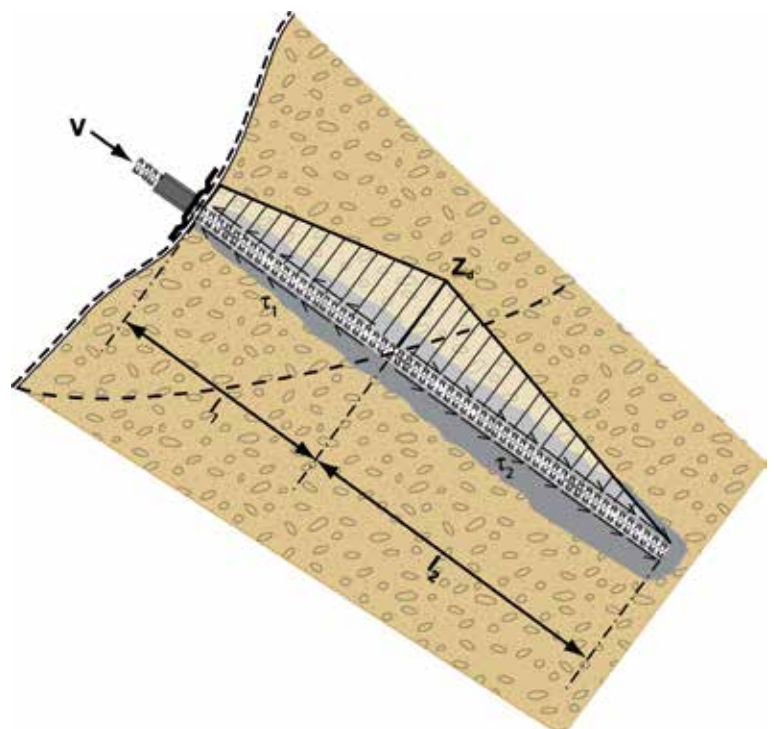
Fig. 26 (right): Load distribution over the nail length

TESTS TO DETERMINE THE BEARING RESISTANCES OF THE SYSTEM.

The following types of bearing resistances of the mesh must be known to permit establishing the proofs of bearing safety for soil and superficially highly weathered and loosened rock slopes:

- ▶ Z_R: Bearing resistance of the mesh against selective tensile stress parallel to the slope
- ▶ D_R: Bearing resistance of the mesh against puncturing in nail direction
- ▶ P_R: Bearing resistance of the mesh against shearing-off at the edge of the spike plate due to a body sliding out of the slope

The bearing resistances of the high-tensile TECCO® steel wire mesh have been determined under the supervision of the Landesgewerbeanstalt (LGA) Nürnberg, Germany with the aid of the testing devices shown in Figs. 27 and 28. These devices have been developed by Rüegger Systems Ltd in cooperation with Geobrugg AG.

Fig. 27: Test setup to determine the bearing resistance of the mesh against selective tensile stress parallel to the slope

Fig. 28: Test setup to determine the bearing resistance of the mesh against puncturing in nail direction

LARGE-SCALE FIELD TESTS.

Goals

The overarching goal for the execution of large-scale field tests was to analyze and better under-stand the load bearing capacity of this type of slope stabilization system under different limiting conditions and under conditions which are as real as possible. This was done with view to the optimal application of such systems in practice. Only instabilities close to the surface with a maximum thickness of 1.20 m were examined in this research project. The overall stability and thereby the dimensioning of the nail anchoring system to prevent fracture mechanisms with low-lying sliding surfaces will not be discussed.

Testing equipment

The testing equipment consists of a 13 x 15 m steel frame which can be filled with soil material through a 10 x 12 m surface up to a layer thickness of 1.20 m. The incline of the frame can vary between 0° and 85° by lifting it with a 500 to crane. The base and side areas of the test area are covered flat with rough wooden planks. To ensure that the sliding surfaces of instabilities close to the surface form within the filling material and do not follow the board floor, wooden slats with a cross sectional area of 30 x 60 mm were applied to increase roughness in the transverse direction. The mesh cover was sewn to upper and lower edge ropes. Depending on the safety system, they exhibit a diameter of 14 - 22 mm and are braced against laterally positioned bollards. To create a cut-out from an infinitely long slope which is as realistic as possible, the mesh cover was screwed to the side of the frame using U-profiles. This created a bedding which was immovable in the lateral direction. GEWI D = 28 mm or D = 32 mm with solidified cladding tubes were used as nails. The connection to the framework construction was made with a base plate welded to the nail which was itself screwed onto another steel plate. The cladding tube was led into a steel tube fastened to the base plate. The nail is considered bend-proof in its connection to the frame. Conventional solidification of the nail was not possible due to reasons concerning the installation and time frame.

Spike plates adjusted to the mesh were used to fasten it. The upper support cable was not held up with nails; instead, it was fastened against bollards using fixing ropes. The lateral distance between the bollards corresponded to the respective horizontal distance between the nails. The mesh webs exhibited widths of 2.0 to 3.5 m and were connected to one another in a force-locking manner via system-specific connectors. To prevent the non-compacted gravel from falling out between the mesh, a mesh with an opening width of 20 x 20 mm with low-tensile strength and no static function was laid out under the mesh cover starting with the 4th test.

Fig. 29 (above): Test no. 13, TECCO® G65/4 + P33, after dismantling mesh cover and removing material, nail grid 3.5 x 3.5 m

Fig. 30 (right): Total overview of testing equipment

Measurement equipment

The surface including nail heads and steel frames were scanned flat using laser scans to serve as a reference level. White cones set on the nails and various mirrors served as orientation aids and reference points. The scan was repeated after changing the incline by 5° each time. Image 31 shows a cross-fade of individual scans. A pendulum and an automatic inclinometer are used to determine the inclination of the steel frame.

The displacements of the top middle nail were measured via a rope potentio-meter to verify the scan data and monitor the deformation during the test. In addition, the forces in the upper and lower support wire ropes were determined using load cells specially adapted to the conditions.

Information on developments in selected nails during changing conditions was gathered using strain gauges. Analyzing this would go beyond the scope of this article. A dissertation will provide a detailed analysis.

Test results

The large-scale field tests also show the positive influence of the installation of the spike plates in previously-created recesses. Creating troughs makes it possible to actively stretch the mesh during installation. This significantly reduces deformations when lifting the steel frame, which makes a significant effect on the load bearing capacity of the entire system.

Verification of RUVOLUM® dimensioning concept

The RUVOLUM® dimensioning concept was developed on the basis of many years of experience in the area of flexible slope stabilization systems and was verified in 2008 using only model tests. The large-scale field tests performed in the scope of the CTI research project make it possible for the first time to examine the theoretical model approach and the underlying assumptions under realistic conditions and using repeatable tests. The graphic analysis of the laser scan shows good agreement with the model approach in accordance with the RUVOLUM® concept. Comparative calculations are now to be perfor-med. The results of the back-calculation correlate quite well with the situation in which the first instabilities close to the surface were observed. If all partial safety factors are set to 1.00 and if the nail inclination is assumed to be per-pendicular to the slope surface as before, the break is calculated to occur and matches very well with the test results.

Conclusions

The large-scale field tests performed create an ideal foundation for a better understanding of the load bearing capacity of flexible slope stabilization sys-tems as well as for further developing them and adapting them to project-specific requirements.

The size of the test frame seems to have been well-selected for simulating instabilities near the surface. In supplementary tests, additional results on impacts to the nails and especially in the nail head area will be gathered. It was possible to verify the RUVOLUM® dimensioning concept.

The results agree well with the test results and the experience gathered over the last 15 years. They are based on a model approach which illustrates the real conditions in a simplified but sufficiently exact manner.

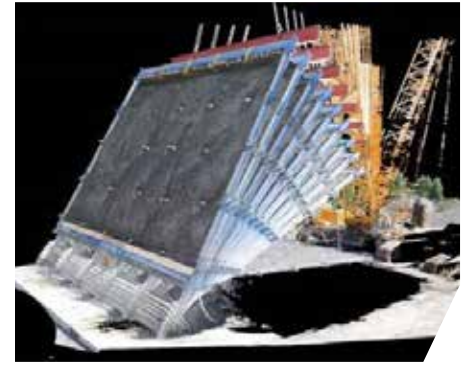

Fig. 31: Test no. 4, TECCO® G65/3 + P33, cross-fade of in-dividual scans

Fig. 32: Test no. 5, TECCO® G65/3 + P33, = 85°, sandy gravel 0 - 63 mm

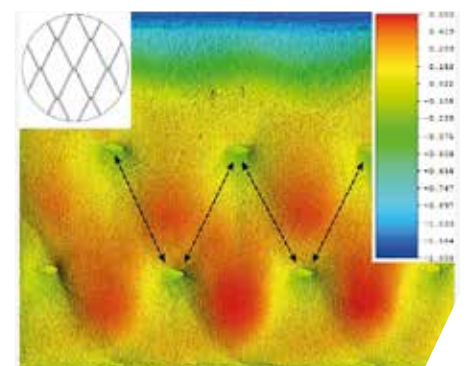

Fig. 33: Test no. 14, TECCO® G65/3 + P66, nail grid 3.5 x 3.5 m, round gravel 16 - 32 mm, $\alpha = 60°$

Fig. 34: Test no. 11 TECCO® G65/3 + P33, nail grid 3.5 x 3.5 m, sandy gravel 0 - 63 mm, $\alpha = 53°$, first slides close to the surface

PROJECT MÜLHEIM, GERMANY

Project data:

Stabilized area	5'000 m²
Stabilization system	TECCO® G65/3, Spike plate P33
Used nail type....................................	GEWI D = 28 mm
Average nail length	4.0 m
Client	City Mülheim / Ruhr, Mülheimer Green and Forest, Germany
Engineering..	Rüegger Systems AG, St. Gallen, Switzerland
Nailing and installation	Landeck GmbH, Rock Protections, Würzburg, Germany
Greening	Eberle Landscaping AG, Herisau, Switzerland
Date of system installation	Spring 2000

Geotechnical parameters in the decomposed superficial area of the subsoil (colluvium / rock):

Friction angle	φ'_k = 28 / 36 degrees
Cohesion	c'_k = 0 kN/m²
Volume weight	γ'_k = 20 / 23 kN/m³

Maximum nail distances:

Inclination of slope	α	45° –70°	
Nail distance horizontal	a	3.30 m	2.50 m
Nail distance in line of slope	b	3.00 m	2.50 m

Project description ....

In Mülheim, Germany, at the Mendenerstrasse on the right-hand bank of the river Ruhr at the foot of the Kahlenberg, a soil and rock slope of approx. 445 m length and maximum 12 m height was secured against rock fall as well as superficial instabilities, and subsequently greened. This work was carried out in spring 2000. To stabilize the surface, the high-tensile steel wire mesh TECCO® developed by Geobrugg AG, Protection Systems, Romanshorn, Switzerland, was used in combination with nailing.

When the road was built along the foot of the slope above the bank of the Ruhr, the natural terrain of the slope was cut steeply. The rock (sandstone, siltstone, clay stone) was laid open over a length of approx. 445 m. The cut slope is 8–12 m high and inclined by 55–75°. Above the cut edge the terrain becomes flatter and the rock is covered by scree and colluvium, respectively.

In January and February 1999, areas of rock broke out repeatedly and slides close to the surface occurred in this cut slope, with the effect that the Mendenerstrasse had to be blocked to the road traffic for safety reasons. Numerous slants and bowed grown trees as well as ground cracks in the forest track with openings as wide as several centimeters above the cut slope pointed to progressive creeping of the superficial layer. Deep slides could be excluded in view of the geological situation.

The soil and rock slope was cleared, cleaned and protected by means of a TECCO® mesh cover in combination with nailing. The general cross-section shows the protection measure that was implemented. Excessively steep areas of scree and colluvium were removed and leveled.
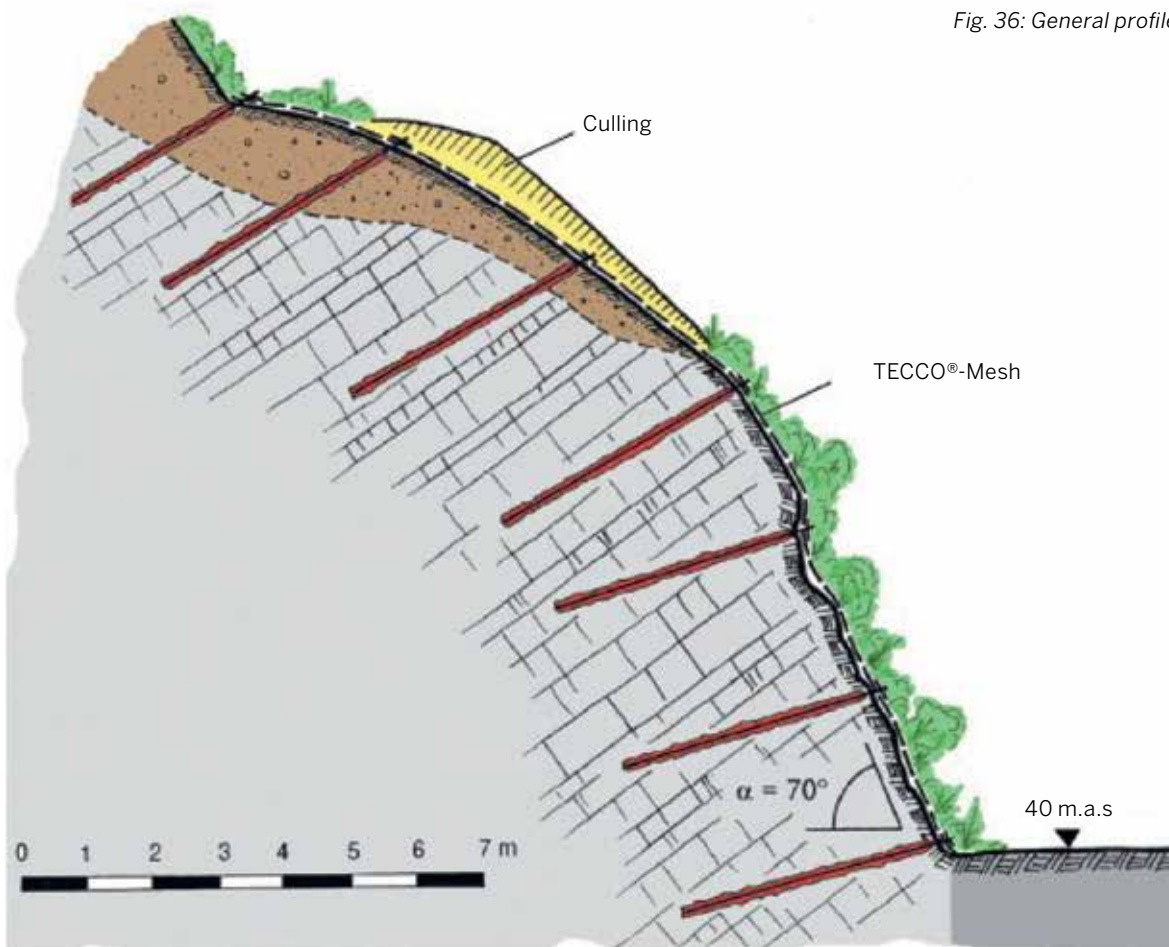
Fig. 35: Sliding

Fig. 36: General profile

Culling

TECCO®-Mesh

α = 70°

40 m.a.s

0 1 2 3 4 5 6 7 m

Fig. 37: Cleaning work

Fig. 38: Drilling work

Fig. 39: Laying of the mesh sheets

Fig. 40 (right): Protected slope in raw state

The TECCO® mesh is held in place by the TECCO® system spike plates and the nailing. By tightening the GEWI nuts, the system spike plates and thereby the mesh are firmly pressed onto and in some cases slightly into the subsoil at a defined force. This permits to actively and largely prevent deformations in the subsoil, sliding and breaking out of material and to increase the safety and efficiency of the system.

Thanks to the high mechanical strength of the mesh and the optimal interaction between mesh and system spike plates it was possible to realize nail distances of 2.5 m (in the steeper cut section) to max. 3.3 m (in the upper, flatter section) measured horizontally and in the line of slope. Nails of type GEWI D = 28 mm were used for the nailing. The mean nail length is 4.0 m. The TECCO® slope stabilization system was dimensioned on the basis of the RUVOLUM® concept

The protected slope was then greened with the FIBRATER system of Eberle Landschaftsbau AG, Herisau, Switzerland. This system is based on a special, fibre-reinforced vegetation layer which can be applied analogously to sprayed concrete, in one operation and in a layer thickness that suits the particular circumstances. Only a few hours after spraying-on the layer is already stable against erosion even in case of intensive rainfall.

Fig. 41: Upper part of the stabilized area

Fig. 42: Protected rock slope

Fig. 43 (above): Approx. two months after re-vegetation
Fig. 44 (left): 15 years after installation

REVEGETATION/EROSION PROTECTION WITH TECMAT® AND TECCO® GREEN.

Revegetation with TECMAT® erosion protection mat

In steep slopes featuring fine-grained, non-cohesive loose rock or severely weathered rock there is a danger of erosion. Such fine material can be washed through the TECCO® mesh and flushed away underneath it. Hereby channels and hollows may be formed under the mesh.

The cause is emerging hillside, layer or fissure water, or in otherwise dry slopes also drain water from heavy rainfalls. Emerging hillside, layer or fissure water must generally be captured and drained. Permanent water out- flows will always lead to problems and must be coped with before the slope stabilization measure is started, since corrective action is hardly possible afterwards. Particular care must also be taken that no larger quantities of surface water from above flow over the slopes. If appropriate, drain channels must be provided above the edge of the slope so that the water is drained to the side in a controlled manner.

What remains is the rainwater falling directly onto the protected slope. In case of a high intensity and long duration of the rain this can also lead to erosion problems. The impact of the rain drops and the draining water may lead to soil movements, flushing-away and general erosion. The problem can be coped with by means of a full-surface vegetation face. The roots stabilize the surface layer and a substantial quantity of water is stored in the vegetation layer before it starts to flow off.

However, it takes time for an effective vegetation to form and for stable subsoil circumstances to result also in the small sphere. No vegetation can develop in a slope subject to movements and erosion. Immediate spraying of erosion-resistant vegetation material and seeding are not always possible directly after laying of the meshes (vegetation period). It is often necessary, therefore, to provide an erosion protection together with the mesh so that erosion and washing-out are prevented for the time being and optimal prerequisites achieved for successful greening later on.

Fig. 45 (above):
High-tensile steel wire mesh TECCO®

Fig. 46 (right):
TECMAT® erosion control mat

Regrettably it is usually not possible to achieve the goal with the known erosion protection mats of natural fibres (jute, choir) because the often irregular surfaces prevent an uninterrupted ground contact of the mats. The mats in question are normally too tight for spraying-through of vegetation material and seeds. The results are undesirable and in the long run critical bare patches which expose the free surfaces to erosion again as soon as the mats have rotted away.

What was sought, therefore, was a flexible mat of a three-dimensional open structure which provides a comparatively good protection against erosion despite relatively large openings. The mat must also be suitable as an adhesion and stabilization layer for the vegetation for as long as the latter is unable to perform this function. Of importance is also that the mat is optically inconspicuous, i.e. adapted in its color to the substrate.

After various suitability tests with different products, with dry and wet greening also in extreme locations exposed to the south, a three dimensional mat of a loop structure, a so-called random-laid nonwoven fabric of polypropylene was eventually found which meets the partly opposing requirements of erosion protection and vegetation face in optimum manner. The technical data compiled in table 9 apply to this erosion protection mat, developed especially for use in combination with the TECCO® stabilization system and available under the trade name of TECMAT®.

Table 9: Characteristics of TECMAT®

Characteristics of TECMAT®	
Raw material	Polypropylene
Fibers	Extruded monofilaments
Structure	Irregular loopy structure
Thickness	18 mm
Weight	approx. 600 g/m2
Void space	> 95%
Color	Curry-Green

Revegetation with integrated erosion protection mat TECCO® G65/3 GREEN
Alternatively to the TECMAT® Erosion Control Mat the TECCO® G65/3 GREEN can be used where the erosion control mat is already integrated in the mesh.

Table 10:
Characteristics of TECCO® GREEN

Fig. 47 (below):
TECCO® GREEN G65/3

Characteristics of TECCO® GREEN	
Raw material	Polypropylene
Fibers	Extruded monofilaments
Structure	Irregular loopy structure
Thickness	14 mm
Weight	approx. 400 g/m2
Void space	> 90%
Color	Curry-Green
Width/length of roll	3.9 x 25 m
Weight per roll	200 kg

SOLUTION FOR AGGRESSIVE ENVIRONMENT: TECCO® G65/3 STAINLESS.

For very demanding environments such as installations at the coastal area close to the sea, subsoil with low ph-value, acid environment or sulphur in the ground, a slope stabilization with better corrosion protection should be considered. With a TECCO® System in stainless steel quality a sufficient lifetime can be reached. Therefore, the TECCO® G65/3 is produced out of sea water resistant stainless steel quality 1.4462 (AISI 318).

Fig. 48: Installation TECCO® G65/3 STAINLESS Parton Back of Rocks, United Kingdom

Characteristics of TECCO® G65/3 STAINLESS	
Wire diameter	3 mm
Tensile strength of steel wire	≥ 1'650 N/mm²
Tensile strength of steel wire mesh	≥ 140 kN/m
Diagonal	83 x 143 mm
Mesh width	65 mm
Number of meshes transversal	12 pcs./m
Number of meshes longitudinal	7 pcs./m
Weight per m²	1.65 kg/m²
Corrosion protection	STAINLESS (INOX) 1.4462 (AISI 318)

Table 11: Characteristics of TECCO® G65/3 STAINLESS

REFERENCES

[1] *Landslides, Investigation and Mitigation, Special Report 247.*
Transportation Research Board, National Research Council. National Academy Press, Washington, D. C. 1996

[2] Rüegger, R.; Flum, D.; Haller, B.:
Hochfeste Geflechte aus Stahldraht für die Oberflächensicherung in Kombination mit Vernagelungen und Verankerungen.
Technische Akademie Esslingen, Beitrag für 2. Kolloquium „Bauen in Boden und Fels", Januar 2000

[3] Wittke, W.; Erichsen, C.:
Standsicherheitsuntersuchungen auf der Grundlage der Mechanik starrer Körper
GrundbauTaschenbuch, Teil 1: Geotechnische Grundlagen, 6. Auflage, Januar 2001

[4] Kühne, M.; Einstein, H. H.; Krauter, E.; Klapperich, H.; Pöttler, R.:
International Conference on Landslides, Causes, Impacts and Countermeasures.
Davos, Switzerland, 17 – 21 June 2001

[5] Rüegger, R.; Flum, D.:
Slope Stabilization with High performance Steel Wire Meshes in Combination with Nails and Anchors.
Int. Symposium, Earth Reinforcement, IS Kyushu, Fukuoka, Japan, November 1416, 2001

[6] Rüegger, R.; Flum, D.; Haller, B.:
Hochfeste Geflechte aus Stahldraht für die Oberflächensicherung in Kombination mit Vernagelungen und Verankerungen (Ausführliche Bemessungshinweise).
Technische Akademie Esslingen, Beitrag für 3. Kolloquium „Bauen in Boden und Fels", Januar 2002

[7] Rorem, E.; Flum, D.:
TECCO® High-tensile Wire Mesh & Revegetation, System for Slope Stabilization.
International Erosion Control Association, IECA's 35th annual conference. Philadelphia, USA, February 16 – 20, 2003

[8] Flum, D.; Rüegger, R.; Guasti, G.:
Dimensionamento di sistemi di consolidamento flessibili superficiali costituiti da reti in acciaio ad alta resistenza in combinazione a elementi di ancoraggio in barra.
GEAM – Associazione Georisorse e Ambiente Torino, Bonifica di versanti rocciosi per la protezione del territorio, Trento, Italia, 11 – 12 marzo 2004

[9] Rüegger, R.; Weingart, K.; Bickel, M.:
Flexible Oberflächenstabilisierungssysteme aus hochfesten Drahtgeflechten in Kombination mit Boden und Felsnägeln, 3 Fallbeispiele.
Technische Akademie Esslingen, Beitrag für 4. Kolloquium „Bauen in Boden und Fels", Januar 2004

[10] Flum, D.; Rüegger, R.:
Dimensioning of flexible surface stabilization systems made from high-tensile steel wire meshes in combination with nailing and anchoring in soil and rock.
IX International Symposium on Landslides, Rio de Janeiro, Brazil, June 2004

[11] Rüegger, R.; Flum, D.:
Anforderungen an flexible Böschungsstabilisierungssysteme bei der Anwendung in Boden und Fels
Technische Akademie Esslingen, Beitrag für 5. Kolloquium „Bauen in Boden und Fels", Januar 2006

[12] Flum, D.; Zueger, M.; Mrozik, M.:
Stabilization of a 30 m deep cutting along the highway A63 Kaiserslautern – Mainz, Germany, with a flexible slope stabilization system consisting of hightensile steel wire mesh in combination with nailing.
Autostrada Polska, Kielce, Poland, May 2006

[13] Flum, D.; Rüegger, R.:
Dimensioning of flexible surface stabilization systems made from high-tensile steel wire meshes in combination with nailing and anchoring in soil and rock.
XIII. DanubeEuropean Conference on Geotechnical Engineering, Ljubljana, Slovenia, May 2006

[14] Cała M., Stolz M., Rist A., Baraniak P., Roduner A.
Large scale field tests for slope stabilizations made with flexible facings.
Proceedings of Eurock 2013. Wrocław, Poland 23-26 September 2013:659-662

[15] Baraniak P., Schwarz-Platzer, K., Stolz, M., Shevlin, T., Roduner, A.
Large scale field tests for slope stabilizations made with flexible facings.
Kingston, GEOHAZARDS 6, 2014

GEOBRUGG®
BRUGG

Safety is our nature

Your local Geobrugg specialist:
www.geobrugg.com/contacts